ACTA ASTRONOMICA
Vol. **0** (2000) pp. 0–0

Petersen diagram for RRd stars in the Magellanic Clouds

by

B. L. Popielski [1], W. A. Dziembowski [1,2] and S. Cassisi [3]

[1] Warsaw University Observatory, Al.Ujazdowskie 4, 00-478 Warsaw, Poland
[2] Nicolaus Copernicus Astronomical Center, ul.Bartycka 18, 00-716 Warsaw, Poland
[3] Osservatorio Astronomico Collurania, I-64100, Teramo, Italy
e-mail: popielsk@astrouw.edu.pl, wd@astrouw.edu.pl, cassisi@astrte.te.astro.it

Received 2000

ABSTRACT

RRd stars from the Magellanic Clouds form a well-defined band in the Petersen diagram. We explain this observed band with our evolutionary and pulsation calculations with assumed metallicity [Fe/H]$= (-2, -1.3)$. Vast majority of RRd stars from LMC is confined to a narrower range of $(-1.7, -1.3)$. The width of the band, at specified fundamental mode period, may be explained by mass spread at given metallicity. The shape of the band reflects the path of RRd stars within the RR Lyrae instability strip. We regard the success in explaining the Petersen diagram a support for our evolutionary models, which yield, mean absolute magnitude in the mid of the instability strip, $\langle M_V \rangle$, in the range 0.4 to 0.65 mag implying distance modulus to LMC of 18.4 mag.

Key words: *stars: variable, stars: oscillations, stars: RR Lyrae, stars: double-mode pulsations, galaxies: Magellanic Clouds, stars: abundances*

1. Introduction

RR Lyrae stars are objects of great importance for whole astrophysics. Double-mode RR Lyrae stars (RRd), constitute relatively rare subtype. Nonetheless RRd stars attract considerable attention because they provide us an additional precise observable, which is the second period (see review of Kovács (2000a)).

Usefulness of double-mode pulsators was first realized by Petersen (1973). Following his idea, the period data for double-mode pulsators are commonly represented in diagrams, called now *Petersen diagrams*, in which the period ratio, $\mathcal{R} = P_1/P_0$, is plotted against the fundamental mode period, P_0. Published examples of Petersen diagrams for RRd stars may be found in the following papers: Nemec *et al.* (1985a), Clement *et al.* (1986), Walker *et al.* (1994), Alcock *et al.* (1997,2000b), Beaulieu *et al.* (1997). The Oosterhoff dichotomy is manifested in

Petersen diagrams for RRd stars. Namely, RRd variables from the Oosterhoff I globular clusters occur in systematically shorter period range than those from the Oosterhoff II (Smith 1995).

Petersen diagram in its first application was used to derive mass and radius estimates for Cepheids (Petersen 1978). The result was a huge discrepancy, known as the double-mode Cepheid mass problem, between the masses derived in this way and the evolutionary masses. The problem disappeared once the OPAL opacities became available (Moskalik *et al.* 1992).

First comparison of the observed and theoretical Petersen diagrams for RR Lyrae stars was made by Cox *et al.* (1980). No large discrepancy between observations and models was found. The new opacities were first used to calculate period ratios for RRd models by Cox (1991), later by Kovács *et al.* (1991,1992) and Bono *et al.* (1996). Kovács & Walker (1999) used data on RRd stars from globular clusters to derive luminosities of RR Lyrae stars yielding support for a brighter luminosity scale.

A large number of data on RRd stars became available as a byproduct of microlensing surveys. Most of currently known RRd stars were observed by MACHO collaboration (Alcock *et al.* 1997,2000b). Figure 1. shows Petersen diagrams for all known RRd stars. The objects belonging to different stellar systems, galaxies and globular clusters, are shown in separate panels with big dots. We see that RRd stars form quite a narrow curved band in the Petersen diagram. The objects from LMC are spread all over the period range, which is $0.46 - 0.6$ d. Short period end in LMC is significantly more populated. We don't see such a concentration for the SMC objects which are more-or-less uniformly distributed, however in view of much scarcer data this conclusion must be regarded preliminary. The data for the Galaxy and dwarf galaxies Draco and Sculptor are too sparse to conclude anything about properties of RRd stars in these systems. The objects from globular clusters are localized in small parts of the band.

The goal of our paper is to explain the properties of the RRd band as defined by the objects from LMC and SMC. From this we expect to learn something about RR Lyrae star properties, particularly their luminosities, as well as about early history of star formation in the Magellanic Clouds. Furthermore, the abundant data on RRd stars may yield us a useful constraint regarding the origin of double-mode pulsation. Although the double-mode pulsation has been successfully modeled (e.g. by Feuchtinger (1998)), our understanding of its causes is not yet satisfactory.

Application of Petersen diagrams as a probe of stellar properties is explained in Section 2. In Sections 3. and 4. we provide some details regarding our model and pulsation calculations, respectively. Interpretation of the RRd band based on model calculation are presented in Section 5. In Section 6. we discuss absolute magnitudes of RRd stars. Uncertainties of the theoretical Petersen diagram are analyzed in Section 7.

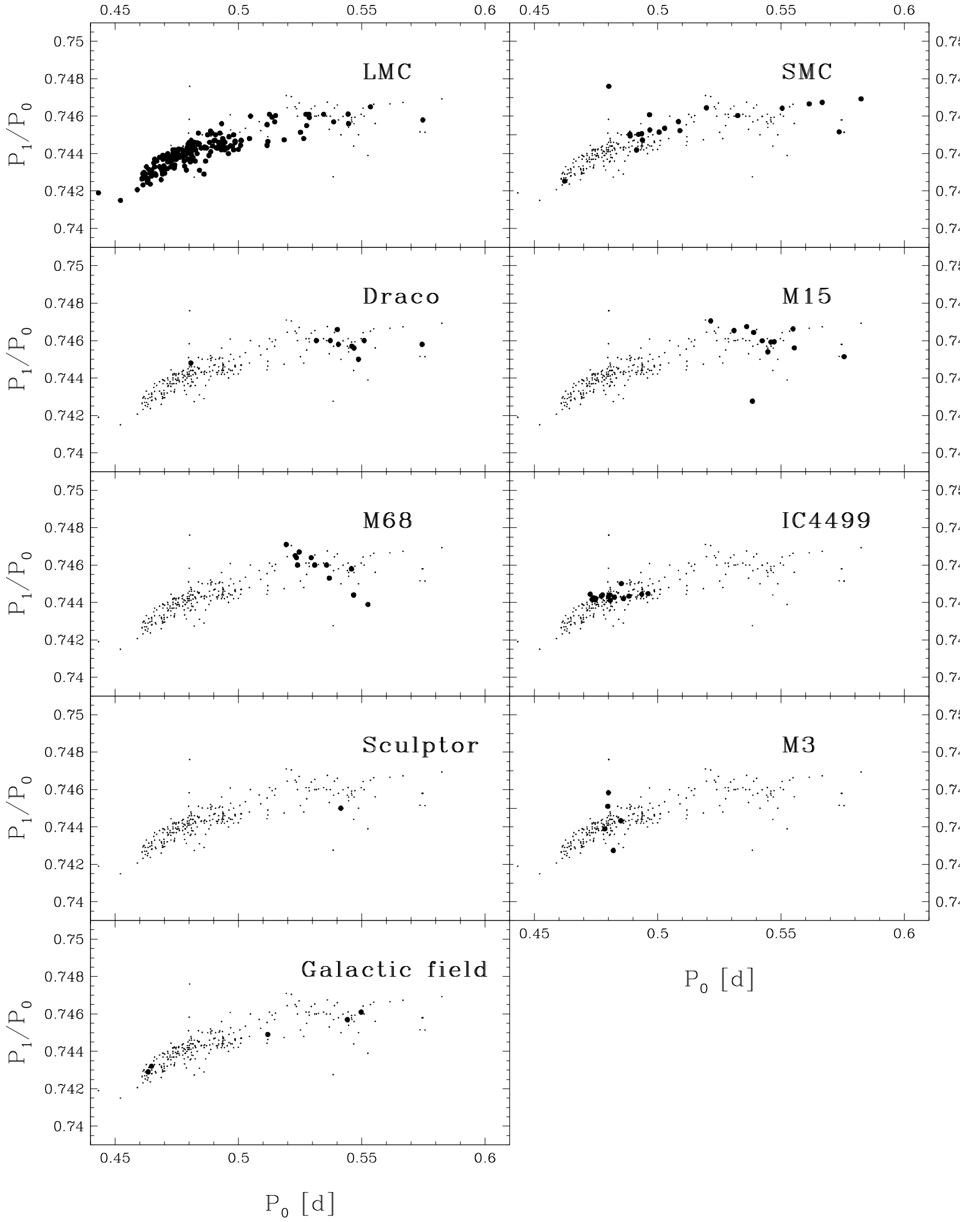

Figure 1: *Petersen diagrams* for RRd stars in various stellar systems. Data taken from (number of objects in parentheses): **LMC** (181) – Alcock *et al.* (1997, 2000b), **SMC** (26) – OGLE private communication (unpublished), **Draco** (10) – Nemec (1985a), **IC4499** (16) – Clement *et al.* (1986), Walker & Nemec (1996), **M3** (5) – Corwin *et al.* (1999), **M15** (12) – Nemec (1985b), Jurcsik & Barlai (1990), Purdue *et al.* (1995), **M68** (12) – Walker (1994), **Sculptor** (1) – Kałużny *et al.* (1995), **Galactic field** (5) – Garcia-Melendo & Clement (1997), Clementini *et al.* (2000).

2. Petersen diagram astrophysics

One needs six parameters to calculate envelope structure and radial mode frequencies. These are, for example: mass, luminosity, effective temperature, two parameters for chemical composition (i.e. Y and Z) and the mixing-length theory parameter (α). We fixed the value of X at 0.76 because possible small variations about such a value have little effect on stellar properties. We also fixed the value of α in our main surveys, however in Section 7. we discuss uncertainties connected with the choice of α. Also in Section 7. we discuss effects of choosing heavy element composition different than the solar mix (Grevesse & Noels 1993) adopted by us as a standard in pulsation calculations. We use this standard to translate Z to [Fe/H]. This quantity is more customary than [M/H].

Figure 2. shows how the four remaining parameters affect position of the RRd model in the Petersen diagram. The reference model may be regarded typical for RRd stars in LMC. We may see that the parameter crucial for the value of period ratio is Z, which is not a new observation. Next important parameter is luminosity, L, and mass, M. However, M and L are strongly constrained by Z, as we will see in next sections. Thus, we may regard the value of period ratio as a probe of metallicity. If we assume that the mass of RR Lyrae star is determined by Z, which is only approximately correct, then with the help of stellar evolution calculations, which yield $L(M, T_{\rm eff}, Z)$ (in fact, two of them because of the shape of the track), we obtain a one-to-one correspondence between a trajectory in the Petersen diagram and the $T_{\rm eff}(Z)$ dependence for RRd stars. In reality, we do not have unique $M(Z)$ dependence, thus we have a band rather than a single trajectory. Still, the shape of the band must reflect primarily the $T_{\rm eff}(Z)$, or equivalently, $L(T_{\rm eff})$ relation for RRd stars.

3. Evolutionary models

All the evolutionary tracks for He-burning stellar models used in the present analysis, have been obtained by means of the FRANEC evolutionary code (Straniero & Chieffi 1989, Cassisi & Salaris 1997, Castellani *et al.* 1999), by adopting canonical semiconvection for the treatment of mixing during the central He-burning phase (Horizontal Branch, hereinafter HB).

The OPAL radiative opacities (Iglesias & Rogers 1996) have been adopted for temperatures higher than $10,000$ K, while for lower temperatures we have used the molecular opacity tables provided by Alexander & Ferguson (1994). This choice allows us to have a smooth match between the two different opacity sets. Both high and low-temperature opacities have been computed by assuming a solar scaled heavy element distribution (Grevesse 1991). As far as it concerns the equation of state, we adopted the Straniero (1988) EOS supplemented at lower temperatures with a Saha EOS. The outer boundary conditions have been fixed according to the

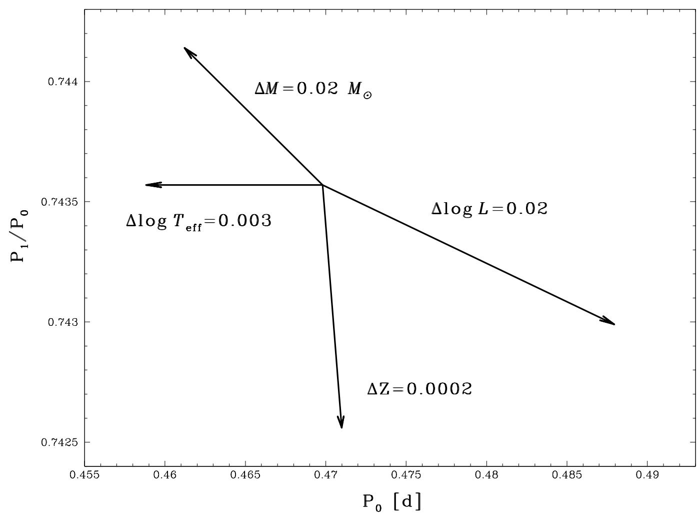

Figure 2: The effect of the envelope parameters on the model position in the Petersen diagram. The central model is characterized by the following parameters: $X = 0.76$, $Z = 0.0007$, $\log T_{\rm eff} = 3.842$, $\log L/L_{\odot} = 1.705$ and $M = 0.69\,M_{\odot}$.

$T(\tau)$ relation given by Krishna-Swamy (1966). Concerning the treatment of the superadiabatic layers the mixing-length calibration provided by Salaris & Cassisi (1996) has been adopted. The other physical inputs are the same as in Cassisi & Salaris (1997).

We have computed evolutionary sequences of models for several metallicities, but by adopting in all cases an initial helium abundance equal to $Y = 0.23$. All the HB models correspond to a Red Giant Branch progenitor with mass equal to $0.8\,M_{\odot}$. In fact, the Zero Age HB structures have been constructed, for each fixed metallicity, by using the helium core mass and the envelope chemical abundance profile suitable for a RGB progenitor with this mass.

4. Pulsations

Our next step was to map evolutionary tracks into Petersen diagram. The envelope models were calculated for surface parameters taken from the evolutionary tracks. The linear non-adiabatic periods were calculated with a standard pulsation code (Dziembowski 1977). The envelopes were calculated with slightly different physics than the evolutionary models. OPAL equation of state was adopted in whole envelope. Although there are very small differences between HB tracks computed with the OPAL compared to Straniero (1988) equation of state, the differences in resulting periods could be significant. The depth of the envelope and the spatial resolution were determined by the accuracy requirement of period ratios on the level of 2×10^{-4}. Convection was treated with standard MLT formalism. In pulsation calculation we ignored the Lagrangian perturbation of the convective

Z	M_{min}	M_{max}
0.0015	0.62	0.675
0.001	0.64	0.695
0.0005	0.665	0.715
0.0003	0.7	0.751
0.0002	0.735	0.785
0.0001	0.79	0.855

Table 1: The allowed masses of RR Lyrae stars in the selected effective temperature range based on the evolutionary tracks.

flux.

We restricted our attention to the central part of the pulsational instability strip, extending from $\log T_{\rm eff} = 3.815$ (6531 K) to 3.855 (7161 K). In this region both fundamental mode and first overtone pulsations are unstable. Feuchtinger (1999) in his numerical simulations found either-or behavior in somewhat narrower temperature range. In another paper Feuchtinger (1998) found a sustained double-mode pulsation at $T_{\rm eff} = 6820$ K.

The segments of the evolutionary tracks from the selected temperature ranges were mapped into the Petersen diagram. Examples are shown in Figure 3.

5. Properties of the RRd band

5.1. Constraints on mass from evolutionary models

Each of our evolutionary tracks is characterized by two parameters, i.e. mass and heavy element abundance of the model (M, Z). Our goal here is to determine range of M for specified Z, corresponding to the selected temperature range (Section 4.). The track is considered allowed if the star spends sufficiently long time, t_s, in this range. Figure 4. shows star lifetimes for models with $Z = 0.0002$ and a range of masses. In Figure 5. we show the total time spent in the selected temperature range (t_s) as function of M and Z. We see that the time depends strongly on M. In the cases of two stays in the selected temperature range, like for $M = 0.74\,M_\odot$ shown in Figure 4., t_s is the sum of two time intervals. For each value of Z we see sharp maxima of t_s (t_s^{max}). The values of M corresponding to the maximum may be described by the following mass-metallicity relation:

$$M/M_\odot = 0.709 - 0.128\,([\mathrm{Fe/H}] + 1.6). \qquad (1)$$

We regarded the M value as allowed if $t_s \geq 0.2\,t_s^{max}$. The range of allowed masses for each Z is given in Table 1.

5.2. *Constraints on metallicity from Petersen diagram*

We have seen in Figure 2. that two parameters most influencing the period ratio value are M and Z. In the previous section we showed that the mass range is significantly limited for given metallicity. Hence, in practice the period ratio determines Z. We can thus determine its ranges by mapping tracks into the Petersen diagram. Figure 3. shows tracks for 3 metallicities and corresponding masses. Mapped tracks allow us to conclude that observed RRd star metallicities range from 0.0002 to 0.001. The resulting RRd "island" in $M-Z$ plane is shown in Figure 6.

We are now in the position to discuss metallicities of RRd stars in the Magellanic Clouds. With the help of Figure 1. and 3.b we may conclude that most of RRd stars in LMC have Z values in the range of $(0.0004, 0.001)$, which translates to [Fe/H]$=(-1.7,-1.3)$. How this value is compared with determinations by others? Kovács (2000a) quotes the [Fe/H] spread of $(-1.9,-1.3)$ for all RRd stars in LMC, what is essentially equivalent to an early estimate of Popielski & Dziembowski (2000). Clementini *et al.* (2000) find a wider range of [Fe/H] from their spectroscopic data for RR Lyrae stars. They quote the $(-2.28,-1.09)$ range. At this point we wish to remind the reader that our [Fe/H] values are inferred assuming the same heavy element abundances as in the sun. Therefore, caution is needed when comparing those values with the spectroscopic ones.

Dolphin (2000) finds evidence for a strong star formation episode at [Fe/H]$=-1.63\pm0.10$ in LMC. The [Fe/H] values for LMC globular clusters containing RR Lyrae stars are in the range $(-2.11,-1.71)$ (Johnson *et al.* 1999). We see in Figure 1. that RRd stars from M3 and IC4499 occur in the region of maximum concentration of RRd stars from LMC. The values of metallicity are respectively -1.57 and -1.5 (Smith 1995), which are close to the center of the metallicity range inferred by us. On the other hand, RRd stars from M15 and M68 occur at the high period end of the RRd band. The metallicities of these two clusters are -2.15 and -2.09 (same source), lower by some 0.2 than those inferred by us. As we discuss in Section 7., this discrepancy may be explained by too low value of α adopted in our pulsation calculation, but also could be due to uncertainty of [Fe/H], which exceeds 0.15 (see for instance Rutledge *et al.* (1997)).

5.3. *Width and shape of the RRd band*

The width of the RRd band at given P_0 may be explained by the mass spread for specified metallicity. The estimate of the corresponding spread in period ratio, $\Delta\mathcal{R}$, is provided in Table 2. We may see that it ranges from 0.002 to 0.004, which is even more than the width of the observed band (see Figure 3.b). In the same figure we may see that the branch ambiguity is a relatively small contributor to the spread in the period ratio.

To simplify further discussion of the shape, we adopt from now on a unique $M(Z)$ relation that is determined by the maxima shown in Figure 5. With this

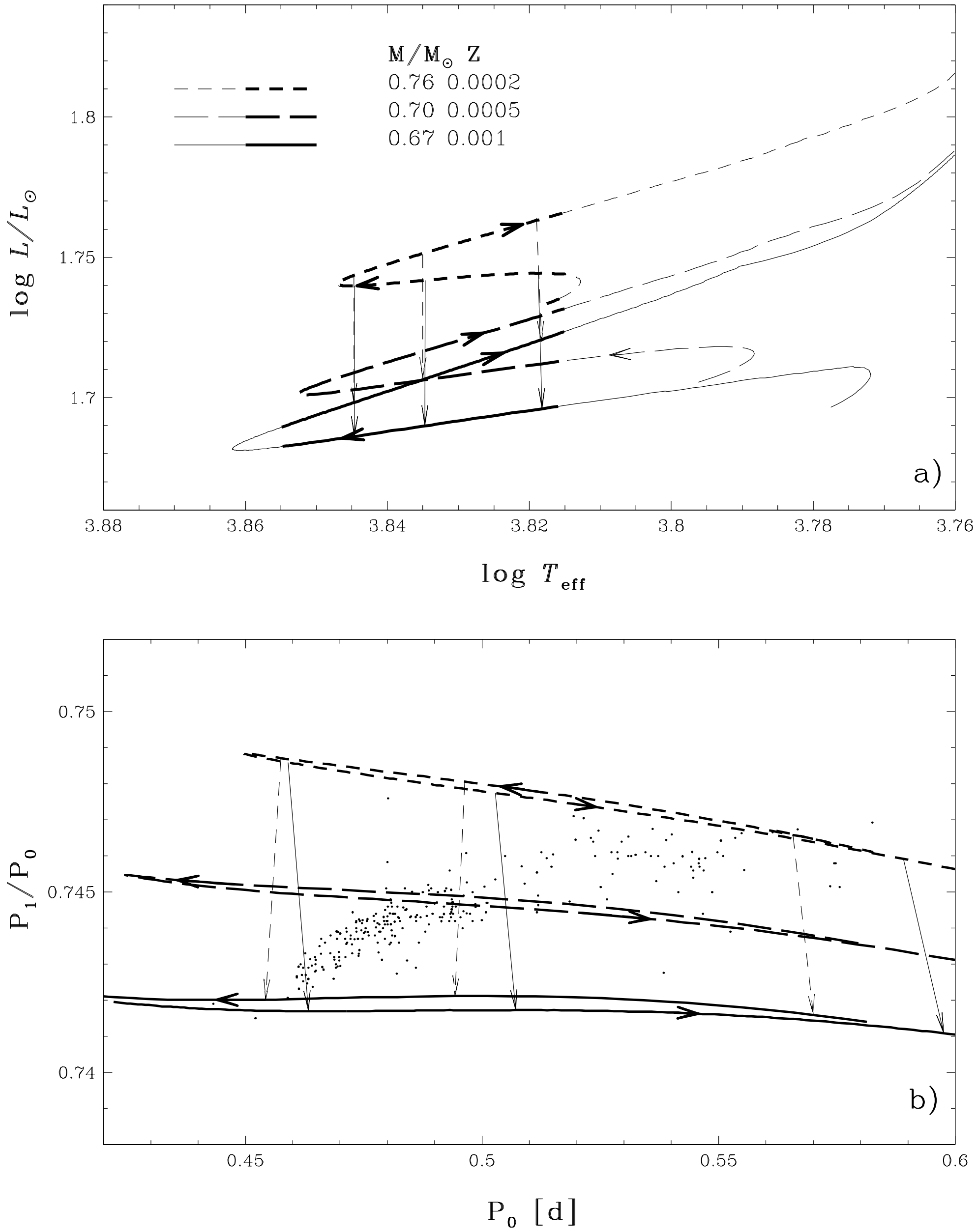

Figure 3: Selected evolutionary tracks in: **a)** *the Hertzsprung-Russel diagram*, **b)** Petersen diagram. In **a)** we use thick lines to denote parts of the tracks used in pulsation calculations. Observed RRd stars are shown as dots in **b)**. Vertical arrows connect models with the same effective temperature, from the left: $\log T_{\rm eff} = 3.845$, 3.835 and 3.818. Solid and dashed arrows correspond to the lower and upper branch of the tracks, respectively.

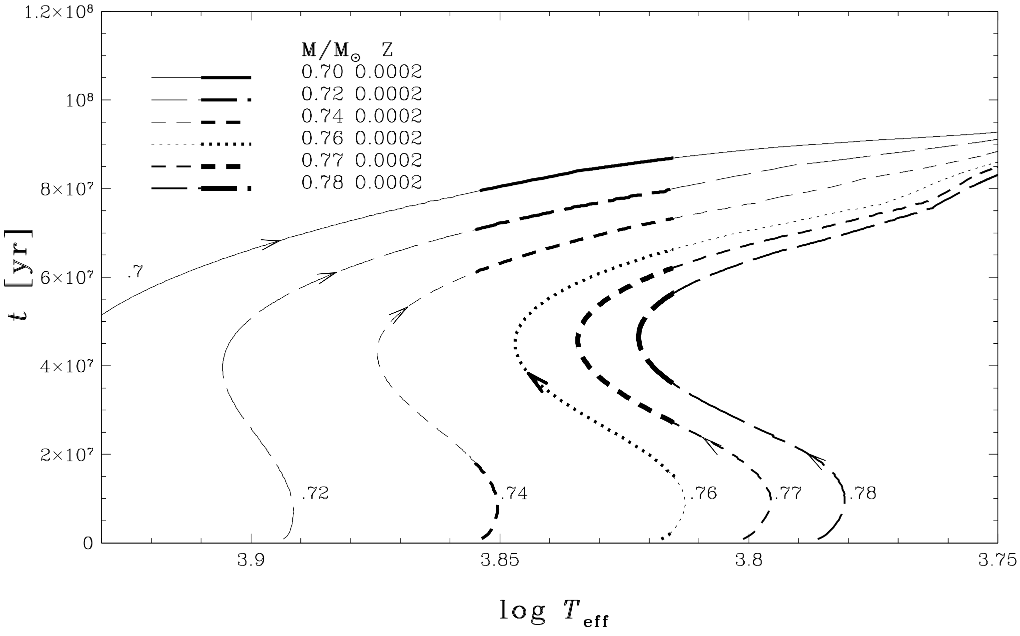

Figure 4: Stellar evolution lifetime from ZAHB versus temperature for different mass RR Lyrae tracks. Lines are thicker within the instability strip.

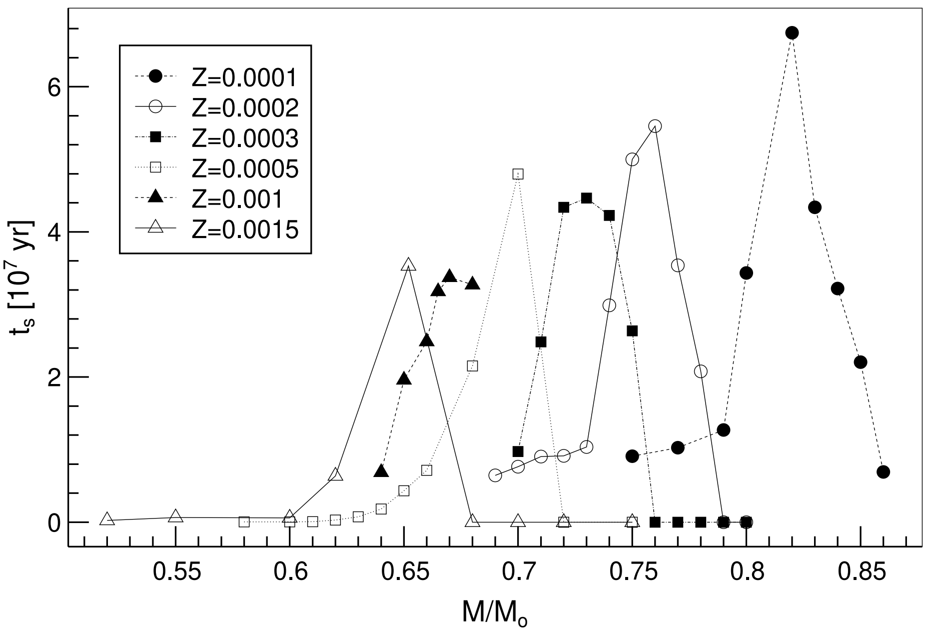

Figure 5: Model evolution lifetime in the selected temperature range for tracks of different mass and Z.

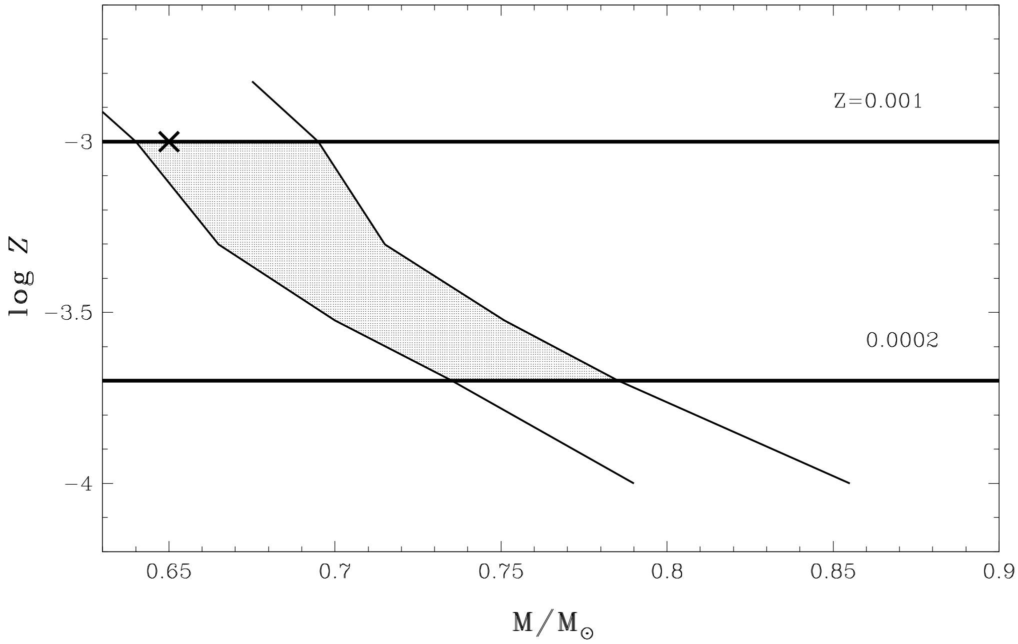

Figure 6: Allowed domain for RRd stars in the $M-Z$ plane. Two sloping $M(Z)$ lines are determined by considering time spent in the selected temperature range. Two horizontal lines follow from the observational Petersen diagram. Nonlinear double-mode model (Feuchtinger 1998) is shown with a cross.

Z	ΔM	$\left(\frac{\partial\mathcal{R}}{\partial M}\right)_{P_0}$	$\Delta\mathcal{R}$
0.001	0.055	0.0667	0.0037
0.0005	0.050	0.0500	0.0025
0.0003	0.051	0.0467	0.0024
0.0002	0.050	0.0428	0.0021

Table 2: Mass spread effect on the Petersen diagram band width at constant P_0.

restriction we may write

$$P_{0,k} = P_{0,k}(Z, T_{\rm eff}), \tag{2}$$

$$\mathcal{R}_k = \mathcal{R}_k(Z, T_{\rm eff}), \tag{3}$$

where $k = 1,2$ identifies the branch of the track. After eliminating $T_{\rm eff}$, we get the Petersen relations $\mathcal{R}_k = \mathcal{R}_k(P_0, Z)$. In Figure 3.b we see that for given Z, the separation reflecting the two choices of k, is well within the observed width. Thus, the shape of the RRd branch reflects the $T_{\rm eff}(Z)$ dependence for RRd stars.

Adopting central values of $\mathcal{R}$ at given P_0, we may invert Eq. (2) and (3) to obtain $T_{\rm eff}(Z)$. In this case, the branch ambiguity is significant. Using our evolutionary tracks and Eq. (1) we found

$$\begin{aligned} \log T_{\rm eff} &= 3.8347 + 0.0363\,([\mathrm{Fe/H}] + 1.6) \quad \text{for the upper branch,} \\ \log T_{\rm eff} &= 3.8315 + 0.0377\,([\mathrm{Fe/H}] + 1.6) \quad \text{for the lower branch.} \end{aligned} \tag{4}$$

Successful nonlinear models of double-mode pulsation should explain these phenomenological relations. At this stage we cannot say whether it is metallicity or luminosity that matters, since the two parameters ($T_{\rm eff}$, [Fe/H]) are correlated. With the use of evolutionary tracks we can determine the corresponding $T_{\rm eff}$ on L relations, which give the locus of RRd stars in the HR diagram. The result is

$$\begin{aligned} \log L/L_\odot &= 1.723 - 2.684\,(\log T_{\rm eff} - 3.835) \quad \text{for the upper branch,} \\ \log L/L_\odot &= 1.703 - 2.124\,(\log T_{\rm eff} - 3.835) \quad \text{for the lower branch.} \end{aligned} \tag{5}$$

These two relations are shown in Figure 7. In the same figure we show lines separating different behavior of RR Lyrae stars from observations and theory.

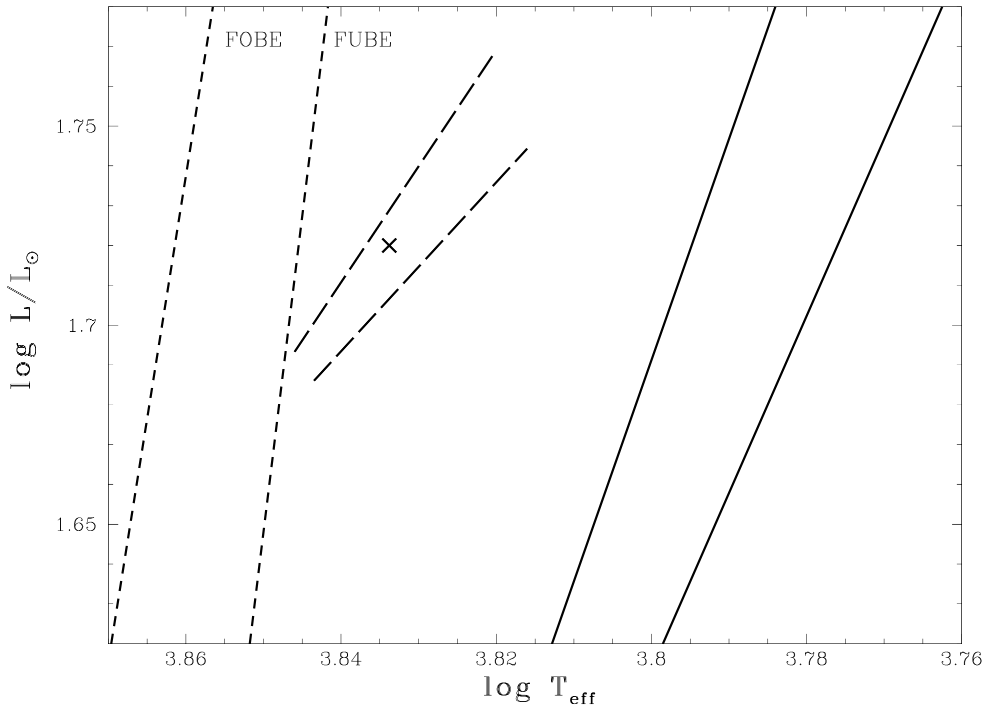

Figure 7: Different pulsational behavior or RR Lyrae in HR diagram. Solid lines encompass observational fundamental mode domain (Géza Kovács - private communication). The two short-dashed lines, which are from model calculations of Kolláth *et al.* (2000), show blue edges for first overtone and fundamental mode pulsators (FOBE and FUBE respectively). The two dashed lines show relations given in Eq. (5). Position of the model for which Feuchtinger (1998) found a sustained double-mode pulsation is shown with a cross.

The RRd localization between RRc and RRab stars was found observationally by Walker (1994) in his work on RR Lyrae in M68. It is supported by recent work of Bakos & Jurcsik (2000) for M3.

It is important to notice that inclination, $-d\log(L/L_\odot)/d\log T_{\rm eff}$, of the bimodality strip is significantly smaller than the inclination of all other characteristic lines shown in Figure 7. According to current understanding, the bimodal behavior is caused by specific property of convection (see e.g. Kolláth & Buchler (2000)). Convection also determines the red edge of the instability strip, thus we would expect a similar inclination of the two lines. That the theory fails to explain inclinations of the characteristic lines is not a new problem. Indeed, as Kolláth *et al.* (2000) pointed out there is a large disagreement between the observational and theoretical lines separating first overtone and fundamental mode pulsators. The bimodality strip from recent model calculations of Kolláth *et al.* (2000) is drastically different than the one determined by us. Apparently, there is still a need for further improvement in nonlinear modeling of RR Lyrae star pulsation.

6. Double-mode pulsators and absolute magnitudes of RR Lyrae stars

Kovács & Walker (1999) used period and photometric data to determine the absolute magnitudes of RRd stars from three globular clusters. This was a novel approach to the important and still vividly debated problem of absolute magnitudes of RR Lyrae stars. Different methods yield results, that may differ as much as 0.3 mag. Kovács & Walker (1999) found RR Lyrae stars brighter by $0.2 \div 0.3$ mag than inferred by means of the Baade-Wesselink method. Their result was amongst those indicating higher luminosity of these stars.

In our investigation we make a different use of RRd stars. Instead of photometric data, we use evolutionary tracks. Following Kovács & Walker (1999) we assume that the luminosities of RRd stars are representative for the whole population of RR Lyrae stars. Choosing evolutionary track at each Z for the central mass value, we may infer L at the RRd temperatures. We recall the [Fe/H] is the customary counterpart of Z, based on Grevesse & Noels (1993). With the help of Kurucz (1999) tabular data, we derived

$$\begin{array}{ll} \langle M_V\rangle = 0.452+0.162\,([\mathrm{Fe/H}]+1.6) & \text{for the upper branch,} \\ \langle M_V\rangle = 0.546+0.240\,([\mathrm{Fe/H}]+1.6) & \text{for the lower branch.} \end{array} \tag{6}$$

The luminosities given in these equations are close to the high luminosity end of the debated range.

Somewhat higher luminosities for RR Lyrae stars were derived by Carretta *et al.* (2000), who relied on the main sequence fitting. He quotes the following result,

$$\langle M_V\rangle = (0.45\pm0.12)+(0.18\pm0.09)\,([\mathrm{Fe/H}]+1.6). \tag{7}$$

Demarque *et al.* (2000) combining their evolutionary tracks with photometric data on globular clusters obtained

$$\langle M_V \rangle = 0.55 + 0.21\ ([\mathrm{Fe/H}] + 1.6), \tag{8}$$

which is not too different from our estimate.

There are three distinct methods which lead to the significantly lower RR Lyrae star luminosities. Gould & Popowski (1998) used the statistical parallax method to infer

$$\langle M_V \rangle = 0.77 \pm 0.13 \text{ at } [\mathrm{Fe/H}] \approx -1.6. \tag{9}$$

Udalski *et al.* (1999) in their determination of the absolute magnitudes relied on the distance to LMC, determined by the red-clump method, and their photometry of RR Lyrae stars. They found the mean value of 0.71 ± 0.07. Smith (1995) quotes two results obtained by means of the Baade-Wesselink method,

$$\begin{array}{ll} \langle M_V \rangle = 0.76 + 0.16\ ([\mathrm{Fe/H}] + 1.6) & \text{after (Jones } et\ al. \text{ 1992),} \\ \langle M_V \rangle = 0.72 + 0.20\ ([\mathrm{Fe/H}] + 1.6) & \text{after (Cacciari } et\ al. \text{ 1992).} \end{array} \tag{10}$$

We should stress however, that more recent analysis of the observational material suggests higher luminosity values

$$\begin{array}{ll} \langle M_V \rangle = 0.63 + 0.21\ ([\mathrm{Fe/H}] + 1.6) & \text{after (Fernley 1994),} \\ \langle M_V \rangle = 0.50 + 0.28\ ([\mathrm{Fe/H}] + 1.6) & \text{after (McNamara 1997).} \end{array} \tag{11}$$

Having determined mean luminosities of RR Lyrae stars we may provide our estimates of distance modulus to LMC. In this we must rely on measurements of visual magnitudes. Mean visual magnitude of RRd stars from the MACHO data is 19.33 mag (Alcock *et al.* 2000a). From Eq. (6), adopting [Fe/H]=-1.5, we get average absolute magnitude of 0.52 mag, which implies $(m-M)_{\mathrm{LMC}} = 18.81$ mag. If instead of MACHO we adopt OGLE mean visual magnitude (Udalski *et al.* 1999), we get $(m-M)_{\mathrm{LMC}} = 18.42$ mag. The OGLE mean value refers to a sample of various types of RR Lyrae pulsators, but we have no evidence, there is a systematic difference in luminosities between RRd stars and the whole population of RR Lyrae stars. These numbers may be compared with $(m-M)_{\mathrm{LMC}} = 18.53$ mag, derived by Kovács (2000a), by means of the method developed by Kovács & Walker (1999). Kovács (2000b) application of a similar method to double-mode Cepheids from SMC implies, after using distance modulus difference between SMC and LMC of 0.51 mag (Udalski *et al.* 1999), $(m-M)_{\mathrm{LMC}} = 18.54$ mag. A recent measurement of the LMC distance modulus based on the Red-Clump method (Romaniello *et al.* 2000), as well as other works based on different distance indicators - referenced therein, supports also a long-distance scale.

7. Uncertainties

We have seen that the Petersen diagram is indeed a powerful tool for diagnosing evolutionary models of RR Lyrae stars and for determining metallicities in stellar systems. The tool, however, requires high precision in calculated period ratios, $\mathcal{R}$. A 10^{-4} difference in the period ratio corresponds to 3% difference in Z. Let us recall that the whole range of period ratios for RRd stars is $0.742 \div 0.748$. It is not difficult to reach the numerical accuracy of 2×10^{-4} in calculated period ratios within the linear non-adiabatic treatment. Typical difference between non-adiabatic and adiabatic period ratios is 0.002.

The treatment of convection has some effect on calculated periods. Undoubtedly, the α effect on $\mathcal{R}$ cannot be ignored. The period ratio values are affected by the difference in the envelope structure implied by change in α. In Figure 8. we illustrate the effect of α on the interpretation of the Petersen diagram. We compare there model results obtained with $\alpha = 1$, which was the adopted standard in our pulsation calculations, with $\alpha = 2$, close to the values adopted in evolutionary track calculations. The choice of $\alpha = 2$ in pulsation calculation implies shift of upper limit of Z from 0.001 to 0.00125 ([Fe/H] from -1.3 to -1.2) and the shift of the lower limit of Z – from

Details of heavy element composition are another effect of potential significance. In our calculations we used the standard solar mixture (Grevesse & Noels 1993). Kovács *et al.* (1992) studied the effect of using different mixtures. Specifically, they considered an oxygen enhanced mixture. Using tabular data of Kovács & Walker (1999) we found that with such a mixture, the maximum value of Z for RRd stars should be about 0.002 instead of 0.001, quoted by us in Section 5.2. However, the change in the metallicity parameter, [Fe/H], isn't high and amounts to about -0.15.

The uncertainty of nonlinear effect on the value of period ratio is the most difficult to estimate. The problem was first investigated by Bono *et al.* (1996) and recently revisited by Kolláth & Buchler (2000). These authors found that the period ratio shift due to nonlinear effect is less than zero, in most cases, and may be as large as -8×10^{-4}. We will use the value of -4×10^{-4}, which corresponds to typical amplitudes of RR Lyrae stars. Thus we have to add a 4×10^{-4} correction to infer the linear period ratio value from observations. This correction translates to 10% decrease in the inferred value of Z (0.05 decrease in [Fe/H]).

8. Summary

We have seen that the Petersen diagram for RRd stars in the Magellanic Clouds may be explained by standard model calculations. The calculations involved evolutionary models of horizontal branch stars and linear non-adiabatic calculations of radial pulsation periods. The agreement has been achieved assuming metal abun-

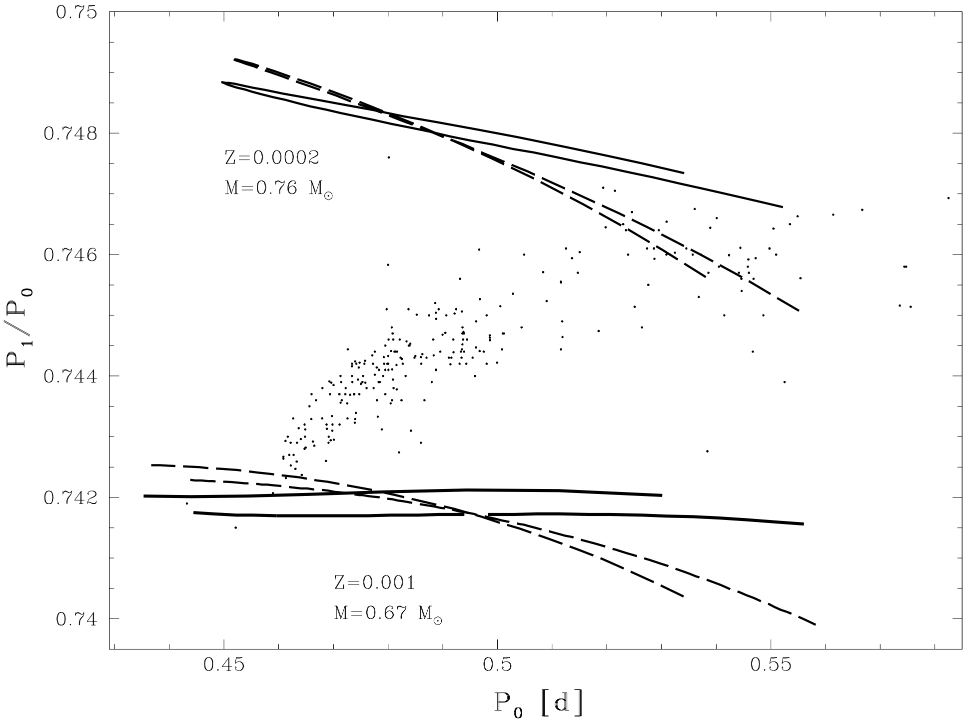

Figure 8: The effect of mixing length theory parameter, α, on model position in the Petersen diagram. Results of pulsation calculations with $\alpha = 1$ (solid lines) are compared with that calculated with $\alpha = 2$ (dashed lines). Dots correspond to RRd data.

dances consistent with other determinations.

This successful explanation of the Petersen diagram may be regarded as a test of our models. These models yield mean absolute magnitudes, $\langle M_V \rangle \approx 0.5$ mag. Hence we support the brighter luminosity scale for RR Lyrae stars.

The range of metallicity needed to explain the whole extent of RRd band is [Fe/H]$= (-2, -1.3)$ for both Magellanic Clouds. While in SMC the objects appear to be uniformly distributed in this range, in LMC we see a strong concentration in the range $(-1.7, -1.3)$.

We have discussed uncertainties in our inference on metallicities following from the uncertainty of calculated values of period ratios. Its primary sources are treatment of convection and nonlinear effects as well as ambiguity of the heavy element abundance. All these effects contribute to uncertainty of [Fe/H] on the level of 0.5. All of them should and can be reduced.

The observed width of the RRd band in the Petersen diagram may be explained by the spread in masses at given metallicity. Petersen diagrams provide a stringent constraint on RRd temperatures. As expected, these temperatures correspond to the mid of the RR Lyrae range. In detail however, there is a difference between our RRd path in the HR diagram and that found by nonlinear modeling. Our RRd strip is significantly more inclined than the blue and red edges of the instability strip. The path from nonlinear simulations has inclination more than 90 degrees.

Acknowledgements. We thank OGLE Team for the unpublished data on RRd stars from SMC and Géza Kovács for discussions. We also acknowledge useful comments of Giuseppe Bono. This work was supported in part by the Polish State Committee for Scientific Research grant 2-P03D-14. One of us (S.C.) was supported by MURST under the project "Stellar evolution".

REFERENCES

Alcock, A., Allsman, R.A., Alves, D., Axelrod, T.S., Becker, A.C., Bennett, D.P., Cook, K.H., Freeman, K.C., Griest, K., Guern, J., Lehner, M.J., Marshall, S.L., Minniti, D., Peterson, B.A., Pratt, M.R., Quinn, P.J., Rodgers, A.W., Sutherland, W., and Welch, D.L. 1997, *Astrophys. J.*, **482**, 89.

Alcock, C., Allsman, R.A., Alves, D.R., Axelrod, T.S., Basu, A., Becker, A.C., Bennett, D.P., Cook, K.H., Drake, A.J., Freeman, K.C., Geha, M., Griest, K., King, L., Lehner, M.J., Marshall, S.L., Minniti, D., Nelson, C.A., Peterson, B.A., Popowski, P., Pratt, M.R., Quinn, P.J., Stubbs, C.W., Sutherland, W., Tomaney, A.B., Vandehei, T., and Welch, D.L. 2000a, *Astron. J.*, **119**, 2194.

Alcock, C., Allsman, R., Alves, D.R., Axelrod, T., Becker, A., Bennett, D., Clement, C., Cook, K.H., Drake, A., Freeman, K., Geha, M., Griest, K., Kovács, G., Kurtz, D.W., Lehner, M., Marshall, S., Minniti, D., Nelson, C., Peterson, B., Popowski, P., Pratt, M., Quinn, P., Rodgers, A., Rowe, J., Stubbs, C., Sutherland, W., Tomaney, A., Vandehei, T., and Welch, D.L. 2000b, *Astrophys. J. (in press)*, astro-ph/0005361.

Alexander, D.R., and Ferguson, J.W. 1994, *Astrophys. J.*, **437**, 879.

Bakos, G.Á., and Jurcsik, J. 2000, *ASP Conf. Ser.*, **203**, 255.

Beaulieu, J.P., Krockenberger, M., Sasselov, D.D., Renault, C., Ferlet, R., Vidal-Majar, A., Maurice, E., Prevot, L., Aubourg, E., Bareyre, P., Brehin, S., Coutures, C., Delabrouille, N., de Kat, J., Gros, M., Laurent, B., Lachieze-Rey, M., Lesquoy, E., Magneville, C., Milsztajn, A., Moscoso, L., Queinnec, F., Rich, J., Spiro, M., Vigroux, L., Zylberajch, S., Ansari, R., Cavalier, F., Moniez, M., and Gry, C. 1997, *Astron. Astrophys.*, **321**, L5.

Bono, G., Caputo, F., Castellani, V., and Marconi, M. 1996, *Astrophys. J., Lett.*, **471**, 33.

Cacciari, C., Clementini, G., and Fernley, J.A. 1992, *Astrophys. J.*, **396**, 219.

Carretta, E., Gratton, R.G., Clementini, G., and Fusi Pecci, F. 2000, *Astrophys. J.*, **533**, 215.

Cassisi, S., and Salaris, M. 1997, *Mon. Not. R. Astron. Soc.*, **285**, 593.

Cassisi, S., Castellani, V., Degl'Innocenti, S., and Weiss, A. 1998, *Astron. Astrophys. Suppl. Ser.*, **129**, 267.

Castellani, V., Degl'Innocenti, S., Fiorentini, G., Lissia, M., and Ricci, B. 1999, *Phys. Rep.*, **281**, 309.

Chieffi, A., and Straniero, O. 1989, *Astrophys. J., Suppl. Ser.*, **71**, 47.

Clement, C.M., Nemec, J.M., Robert, N., Wells, T., Dickens, R.J., and Bingham, E.A. 1986, *Astron. J.*, **92**, 825-843.

Clementini, G., Bragaglia, A., di Fabrizio, L., Carretta, E., and Gratton, R.G. 2000, *ASP Conf. Ser.*, **203**, 172.

Clementini, G., Di Tomaso, S., Di Fabrizio, L., Bragaglia, A., Merighi, R., Tosi, M., Carretta, E., Gratton, R.G., Ivans, I.I., Kinard, A., Marconi, M., Smith, H.A., Wilhelm, R.,Woodruff, T., and Sneden C. 2000, *Astron. J. (in press)*, astro-ph/0006174.

Corwin, T.M., Carney, B.W., and Allen, D.M. 1999, *Astron. J.*, **117**, 1332.

Cox, A.N., Hodson, S.W., and King, D.S. 1980, *Astrophys. J.*, **236**, 219.

Cox, A.N. 1991, *Astrophys. J.*, **381**, L71.

Demarque, P., Zinn, R., Lee, Y.-W., and Yi, S. 2000, *Astron. J.*, **119**, 1398.
Dolphin, A.E. 2000, *Mon. Not. R. Astron. Soc.*, **313**, 281.
Dziembowski, W.A. 1977, *Acta Astron.*, **27**, 95.
Fernley, J. 1994, *Astron. Astrophys.*, **284**, L16.
Feuchtinger, M.U 1998, *Astron. Astrophys.*, **337**, 29.
Feuchtinger, M.U. 1999, *Astron. Astrophys.*, **351**, 103.
Garcia-Melendo, E., and Clement, C. 1997, *Astron. J.*, **114**, 1190.
Gould, A., and Popowski, P. 1998, *Astrophys. J.*, **508**, 844.
Grevesse, N. 1991, *IAU Symp. 145, Evolution of Stars: the Photospheric Abundance Connection, ed. G. Michaud, A. Tutukov, (Dordrecht: Kluwer)*, 63.
Grevesse, N., and Noels, A. 1993, *Phys. Scr.*, **T47**, 133.
Iglesias, C.A., and Rogers, F.J. 1996, *Astrophys. J.*, **464**, 943.
Johnson, J.A., Bolte, M., Stetson, P.B., Hesser, J.E., and Somerville, R.S. 1999, *Astrophys. J.*, **527**, 199.
Jones, R.V., Carney, B.W., Storm, J., and Latham, D.W. 1992, *Astrophys. J.*, **386**, 646.
Jurcsik, J. and Barlai, K. 1990, *ASP Conf. Ser. 11: Confrontation Between Stellar Pulsation and Evolution*, 112.
Kałużny, J., Kubiak, M., Szymański, M., Udalski, A., Krzemiński, W., and Mateo, M. 1995, *Astron. Astrophys. Suppl. Ser.*, **112**, 407.
Kolláth, Z., Buchler, J. R., and Feuchtinger, M. 2000, *Astrophys. J. (in press)*, astro-ph/0001442.
Kolláth, Z., and Buchler, J. R. 2000, *Nonlinear Studies of Stellar Pulsation, Eds. M. Takeuti and D.D. Sasselov, Astrophysics and Space Science Library Series, Kluwer (in press)*, astro-ph/0003386.
Kovács, G. 2000a, *Nonlinear Studies of Stellar Pulsation, Eds. M. Takeuti and D.D. Sasselov, Astrophysics and Space Science Library Series, Kluwer (in press).*
Kovács, G. 2000b, *Astron. Astrophys.*, **360**, L1.
Kovács, G., Buchler, J.R., and Marom, A. 1991, *Astron. Astrophys.*, **252**, L27.
Kovács, G., Buchler, J.R., Marom, A., Iglesias, C.A., and Rogers, F.J. 1992, *Astron. Astrophys.*, **259**, L46.
Kovács, G., and Walker, A.R. Astrophys. J., *1999*, **512**, 271.
Krishna-Swamy, K.S. 1966, *Astrophys. J.*, **145**, 174.
Kurucz, R. L. 1999, *Highlights in Astronomy*, **11**, 646.
Nemec, J.M. 1985a, *Astron. J.*, **90**, 204.
Nemec, J.M. 1985b, *Astron. J.*, **90**, 240.
Nemec, J.M., and Clement, C.M. 1989, *Astron. J.*, **98**, 860.
McNamara, D.H. 1997, *Publ. Astron. Soc. Pac.*, **109**, 857.
Moskalik, P., Buchler, J.R., and Marom, A. 1992, *Astrophys. J.*, **385**, 685.
Petersen, J.O. 1973, *Astron. Astrophys.*, **27**, 89.
Petersen, J.O. 1978, *Astron. Astrophys.*, **62**, 205.
Popielski, B.L., and Dziembowski, W.A. 2000, *ASP Conf. Ser.*, **203**, 276.
Purdue, P., Silbermann, N.A., Gay, P., and Smith, H.A. 1995, *Astron. J.*, **110**, 1712.
Romaniello, M., Salaris, M., Cassisi, S., and Panagia, N. 2000, *Astrophys. J.*, **530**, 738.
Rutledge, G.A., Hesser, J.E., and Stetson, P.B. 1997, *Publ. Astron. Soc. Pac.*, **109**, 907.
Salaris, M., and Cassisi, S. 1996, *Astron. Astrophys.*, **305**, 858.
Smith, H.A. 1995, *Cambridge University Press*, Astrophysics Series.
Straniero, O. 1988, *Astron. Astrophys. Suppl. Ser.*, **76**, 157.
Udalski, A., Szymański, M., Kubiak, M., Pietrzyński, G., Soszyński, I., Woźniak, P., and Żebruń, K. 1999, *Acta Astron.*, **49**, 201.
Walker, A.R. 1994, *Astron. J.*, **108**, 555.
Walker, A.R., and Nemec, J.M. 1996, *Astron. J.*, **112**, 2026.